Small Angle Neutron Scattering Study on Nano-dispersoids in CoCrFeMnNi High-Entropy Alloy

SeungHyeok Chung, Ho Jin Ryu*
Nuclear and Quantum Engineering Department, Korea Advanced Institute of Science and Technology, 291 Daehakro, Yuseong, Daejeon, 34141, Republic of Korea
**Corresponding author: hojinryu@kaist.ac.kr*

1. Introduction

Oxide dispersion strengthened (ODS) alloys considered as a promising structural material due to its excellent high temperature mechanical properties and irradiation resistance [1, 2]. ODSs are distinguished by a microstructure in which nanometer scale dispersoids are homogeneously distributed. The dispersoids contribute to the grain boundary strengthening and dispersoid strengthening of the matrix by pinning the grain boundary and dislocation motions during plastic deformation [3]. Therefore, quantitative characterization of dispersoid in the matrix is very important to evaluatethe mechanical properties of ODS alloys. Transmitted electron microscopy (TEM) and atom probe tomography (APT) made it possible to analyze the chemical properties and crystal structure of dispersoids in atomic and nanometer scale characterization with their high spatial resolution. However, TEM and APT have a limited detection volume of material [4]. Therefore, it is necessary to evaluate the representative properties of the material by analyzing statistical data representative from the whole sample volume along with the significant insight of the chemical compositions and dispersoid structures analyzed by TEM and APT. SANS is a well-established technique, giving a dispersoid size, distribution, and volume fraction in materials at the nanometer scale [5].

In this study, the dispersoids characteristics in ODS-HEAs prepared by two distinctive yttrium addition methods was statistically investigated by SANS. Oxide-dispersoids are studied by means of TEM and high-resolution TEM (HRTEM) to determine the neutron scattering length density of the dispersoids formed in the HEA matrix. The results show a difference in size distribution and volume fraction of the dispersoids according to the powder preparation method.

2. Experimental procedures

The ODS-HEAs are prepared by the powder metallurgical way including cryo-milling and spark plasma sintering processes. To promote the formation of oxide-dispersoid in the HEA matrix, two different powder preparation methods classified by yttrium addition strategy: (1) Y_2O_3 particles are added in atomized CoCrFeMnNi HEA powder during cryo-milling, denoted as Y_2O_3 added-ODS-HEA and (2) solid solution of the metallic yttrium with the elements of CoCrFeMnNi HEA prior to the cryo-milling at the powder preparation stage by gas atomization, denoted as Y-alloyed ODS-HEA. For comparison, the pristine CoCrFeMnNi HEA which has no yttrium addition was also prepared with the same process of ODS-HEA preparation. The mechanical alloying temperature was maintained as 97K using liquid nitrogen. The cryo-milling was conducted with a ball-to-powder weight ratio (BPR) of 10:1 at a rotation speed of 600 revolutions per minute for 24 h. The as-milled powders are subsequently consolidated by SPS at 1173K for 10 min with a constant uniaxial pressure of 50 MPa. The consolidated samples have a cylindrical structure with a diameter of 21 mm and 1 mm in thickness.

Small-angle neutron scattering (SANS) measurements were performed using the extended Q-range small-angle neutron scattering diffractometer (EQ-SANS) at the Spallation Neutron Source (SNS) of Oak Ridge National Laboratory (Oak Ridge, TN). The neutron scattering intensity was collected in the Q-range from 0.002 to 1.8 A^{-1} by using three sample-to-detector distance, 1.3 m, 4 m, and 9 m. The IRENA software package was used to analyze the neutron scattering curves [6].

3. Results and Discussions

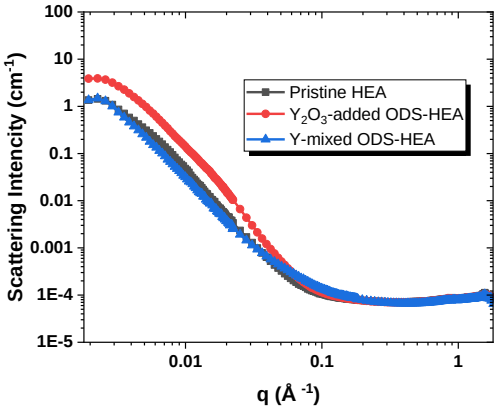

Fig. 1. SANS profiles of the pristine HEA and ODS-HEAs sintered at 1173K

Fig. 1 shows the SANS profiles of the pristine HEA and ODS-HEA sintered at 1173K. In order to carry out the quantitative evaluation of dispersoids, the SANS profiles were fitted assuming that a non-interacting, homogeneously distributed, and spherical dispersoid. A dilute system, in which the HEA matrix and dispersoids were considered as the solvent and solutes, respectively.

For a dilute system with the assumptions, the scattering intensity is given by [6]:

$$I(Q) = |\Delta\rho|^2 \int_0^\infty |F(Q,r)|^2 V(r) f(r) dr \quad (1)$$

where $V(r)$ is the particle volume, $f(r)$ is the volume size distribution of dispersoids, and $|\Delta\rho|^2$ is the neutron scattering contrast given by the square difference in the neutron scattering length density between the matrix and dispersoid. Therefore, the difference in the SANS profiles shown in Fig.1. indicates that the different dispersoid types were formed in the HEA matrix respectively by the different powder preparation methods. The volume fraction and size distribution of dispersoids can be estimated by calculating the neutron scattering contrast, $|\Delta\rho|^2$, as shown in equation (1). The neutron scattering length density is determined by not only the density of scatters but also its chemical composition.

To determine the neutron scattering length density of dispersoids in each alloy, a preliminary TEM study was conducted. Fig. 2 (a) shows an STEM-HAADF image of the pristine HEA. The nano-dispersoids were formed in the HEA matrix even though the yttrium precursor to promote the dispersoid formation was not added. The crystal structure was investigated by the fast Fourier transform (FFT) reflections of the HRTEM image. The FFT reflections indicate the presence of $CrMn_2O_4$ from the $[\bar{3}\bar{1}1]_{\text{tetragonal}}$-zone axis and the matrix was confirmed as a single FCC structure from the FFT reflections as shown in Fig. 2 (c).

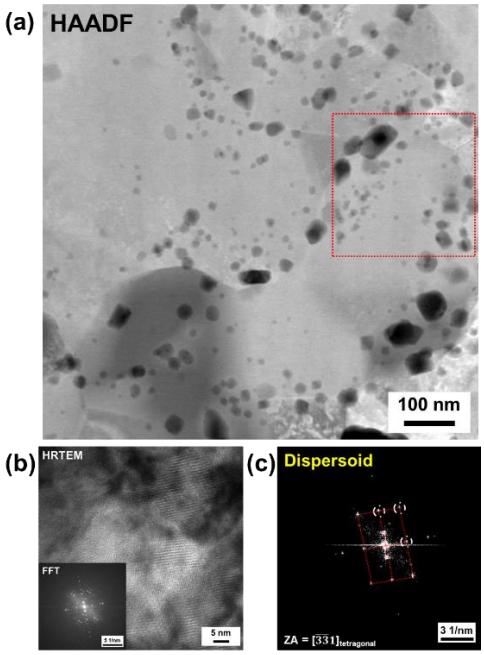

Fig. 2. (a) STEM-HAADF image, (b) HRTEM, and (c) FFT reflection of dispersoid of the pristine HEA

Fig.3 (a) shows an STEM-HAADF image of the Y_2O_3-added ODS-HEA. The relatively coarsened dispersoid with a diameter range of 30–150 nm existed along the grain boundaries, while fine dispersoids are observed inside the grain. The fine dispersoid is a few tens of nanometer or less in diameter. The FFT reflections of the dispersoids inside the grain are identified as Y_2O_3 from the $[001]_{\text{BCC}}$-zone axis as shown in Fig. 3 (c). The coherent interface structure between the dispersoid and matrix was constructed as confirmed from the relationship of crystallographic parallel planes of the dispersoid and matrix. However, the dispersoid formed along the grain boundary has a complex structure with several clusters. The FFT reflections (Fig. 3 (e, f)) indicate that the dispersoid consists of several distinct crystal structures. The FFT reflections from the +1 region reveal the crystal structure of $YCrO_4$ from the $[023]_{\text{Tetragonal}}$-zone axis and the FFT reflections from the +2 region indicate Y_2O_3 from the $[\bar{1}22]_{\text{BCC}}$-zone axis as shown in Fig. 3 (e) and (f) respectively. In contrast to the dispersoid formed inside the grain, the dispersoid formed along the grain boundary has an incoherent interface with the matrix, which may come from the partially-fractured Y_2O_3 particles.

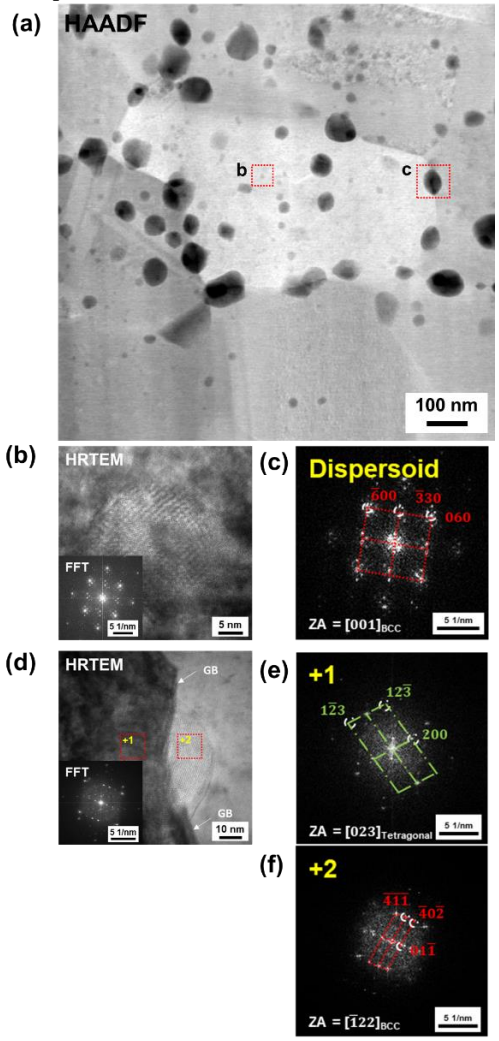

Fig. 3. (a) STEM-HAADF image, HRTEM and FFT reflection of dispersoid (b, c) inside the grain and (d, e, f) along the grain boundary of the Y_2O_3-added ODS-HEA

Fig. 4 (a) shows an STEM-HAADF image of the Y-alloyed ODS-HEA. The dispersoids are in-situ formed

inside the grain and along the grain boundaries with homogeneous dispersoid size. The FFT reflections of dispersoid HRTEM image indicate that the dispersoid has a crystal structure of Y_2O_3 from the $[001]_{BCC}$-zone axis as shown in Fig. 4 (b) and (c). The coherent interface structure between the dispersoid and matrix was constructed as confirmed from the relationship of crystallographic parallel planes of the dispersoid and matrix. It is observed that the coherent interface is formed between the dispersoid and matrix regardless of the location of the dispersoid formed. Due to the homogeneous distribution of dispersoid in the matrix, the nanograined structure was constructed with an average diameter of 330 nm. On the other hands, the grain growth severely occurred in the pristine HEA and Y_2O_3-added ODS-HEA.

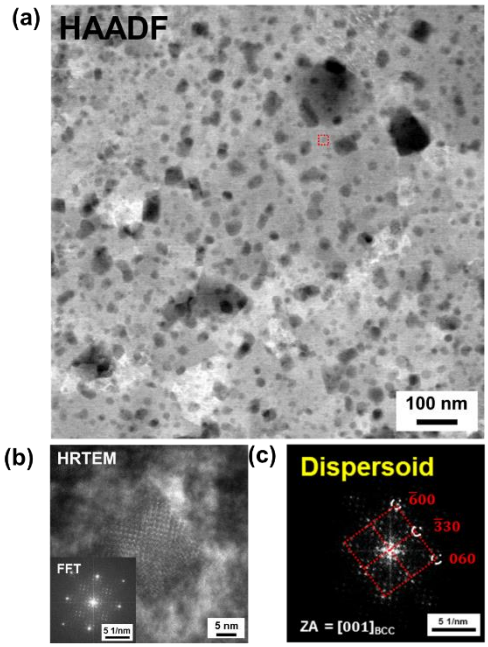

Fig. 4. (a) STEM-HAADF image, (b) HRTEM, and (c) FFT reflection of dispersoid of the Y-alloyed ODS-HEA

To carry out the fitting the SANS profiles for the pristine HEA and ODS-HEAs, Cr-Mn rich dispersoid, and Y rich dispersoid were considered as $CrMn_2O_4$ and $YMn_{0.5}Ni_{0.5}O_3$ respectively. The scattering length densities of $CrMn_2O_4$ and $YMn_{0.5}Ni_{0.5}O_3$ used for the SANS profiles fitting were 2.534×10^{10} cm^{-2} and 5.235×10^{10} cm^{-2} respectively. Fig. 5 shows the volume size distribution of the dispersoids evaluated from SANS profile fitting as a function of the dispersoid diameter. The bimodal volume distribution was observed in all alloys. The evaluated dispersoid diameter and volume fraction are listed in Table 1. The Cr-Mn rich dispersoid in the pristine HEA has relatively larger size than the dispersoid in ODS-HEAs, the coarsening was suppressed compared to Y_2O_3 ODS-HEA. Among the alloys, the bimodal volume distribution was more pronounced in Y_2O_3-added ODS-HEA due to the coarsened dispersoids along the grain boundaries. However, the dispersoids size distribution with a diameter of less than 10 nm is dominantly expressed in Y-alloyed ODS-HEA.

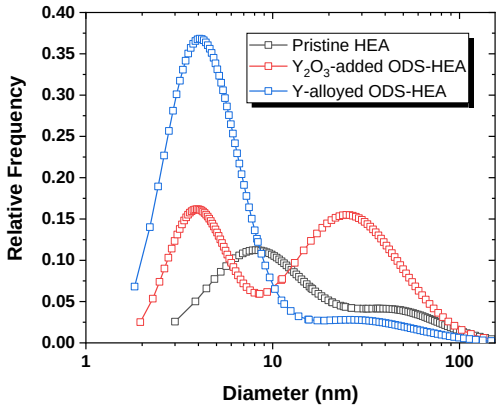

Fig. 5. The volume size distribution of dispersoids evaluated from SANS profile fitting

Table 1. The statistical results on dispersoid diameter and volume fraction of the pristine HEA and ODS-HEAs evaluated by SANS profile fitting

	Dispersoid diameter (nm)		Dispersoid volume fraction (%)	
	Dist. 1	Dist. 2	Dist. 1	Dist. 2
Pristine HEA	8.10	45.28	0.81	1.48
Y_2O_3-added ODS-HEA	3.92	24.79	0.31	3.95
Y-alloyed ODS-HEA	4.07	27.30	0.96	0.94

4. Conclusions

The dispersoid behavior in the pristine HEA and ODS-HEAs prepared by two distinctive yttrium addition methods was investigated by SANS. Especially, the dispersoids having a size of less than 10 nm, which was limited in the analysis was statistically investigated. The nano-dispersoids with Cr and Mn rich composition were confirmed in the HEA matrix despite the yttrium precursor to promote the dispersoid formation that was not added. SANS analysis identified that in-situ dispersoid formation with a coherent interface structure in Y-alloyed ODS-HEA can refine the dispersoid size and grain structure with high dispersoid number density. However, ex-situ dispersoid with incoherent interface formed in Y_2O_3-added ODS-HEA coming from the

partially-fractured Y_2O_3 particles causes coarsening of dispersoids.

ACKNOWLEDGEMENT

The SANS measurements were performed at the Spallation Neutron Source (SNS) Extended Q-Range Small Angle Neutron Scattering (EQ-SANS), Oak Ridge National Laboratory (ORNL). The present work has been supported by Agency for Defense Development (ADD) of Republic of Korea under the contract 1415156504.

REFERENCES

[1] F. Siska, L. Stratil, H. Hadraba, S. Fintova, I. Kubena, V. Hornik, R. Husak, D. Bartkova, T. Zalezak, Strengthening mechanisms of different oxide particles in 9Cr ODS steel at high temperatures, Mater. Sci. Eng. A. 732 (2018) 112–119. https://doi.org/10.1016/j.msea.2018.06.109.

[2] S.J. Zinkle, G.S. Was, Materials challenges in nuclear energy, Acta Mater. 61 (2013) 735–758. https://doi.org/10.1016/j.actamat.2012.11.004.

[3] M. Nagini, R. Vijay, K. V. Rajulapati, A. V. Reddy, G. Sundararajan, Microstructure–mechanical property correlation in oxide dispersion strengthened 18Cr ferritic steel, Mater. Sci. Eng. A. 708 (2017) 451–459. https://doi.org/10.1016/j.msea.2017.10.023.

[4] R. Coppola, M. Klimiankou, R. Lindau, R.P. May, M. Valli, SANS and TEM study of y2O3 particle distributions in oxide-dispersion strengthened EUROFER martensitic steel for fusion reactors, Phys. B Condens. Matter. 350 (2004) 545–548. https://doi.org/10.1016/j.physb.2004.03.148.

[5] International Atomic Energy Agency., IAEA, Small angle neutron scattering, IAEA Rep. 2000-2003. (2006) 113. http://www-pub.iaea.org/books/IAEABooks/7439/Small-Angle-Neutron-Scattering.

[6] J. Ilavsky, P.R. Jemian, Irena: Tool suite for modeling and analysis of small-angle scattering, J. Appl. Crystallogr. 42 (2009) 347–353. https://doi.org/10.1107/S0021889809002222.

[7] M. Mujahid, J.W. Martin, The effect of oxide particle coherency on Zener pinning in ODS superalloys, J. Mater. Sci. Lett. 13 (1994) 153–155. https://doi.org/10.1007/BF00278146.